Propagation Loss Variability due to Hourly Variations of Underwater Sound Speed Profiles in the Korea Strait

대한해협에서 수중음속 구조의 단기변화에 의한 전파손실의 변화정도

Young Nam Na*, Taebo Shim*, Seong Il Kim*
나 영 남*, 심 태 보*, 김 성 일*

ABSTRACT

In order to estimate the variability of the wave propagation loss (PL) due to hourly variations of the sound speed profiles (SSPs), we conducted oceanographic measurements every hour for 39 hours in October 1993 in the Korea Strait. Currents and meteorological data were measured simultaneously to examine the causes of the temporal variations of temperatures. During the experiment, the temporal variations of temperatures in the surface layer highly depend on the water mass transport from adjacent seas. The PL for low frequency (75-300 Hz) is calculated using the parabolic equation scheme and averaged over the whole water depth. The hourly variation of the SSP may cause a PL difference of up to 10 dB over a 30-50 km range. The variability of PL, represented by standard deviation for the 39 SSPs, is as large as 3 dB over a 50 km range.

요 약

수중음속 구조의 시간변화에 기인한 전파손실의 변화정도를 추정하기 위해 1993년 10월 대한해협에서 39 시간 동안 1 시간 간격의 해양학적 관측을 실시하였다. 수온의 시간 변화를 일으키는 요인을 살펴보기 위하여 해류와 기상학적인 관측도 동시에 실시하였다. 관측기간 동안 표층 혼합층에서 수온의 시간 변화는 관측점 주위 해역의 수괴와 밀접하게 관련되어 있다. 저주파 대역(75-300 Hz) 전파손실은 포물선 방정식 기법을 도입한 모델을 이용하여 계산하고 전 수심에 대해 평균을 취하였다. 수직음속 구조의 시간 변화는 30-50 km 거리에서 10 dB 이상의 전파손실 차이를 일으킬 수 있다. 39 개 수직음속 구조에 대한 전파손실의 표준편차 변화정도는 50 km 거리에서 3 dB에 달한다.

I. Introduction

The ocean is an extremely complicated medium for acoustic wave propagation. The most characteristic feature is its inhomogeneous nature. There are two kinds of inhomogeneities, regular and random.[1] They both strongly influence the sound field in the ocean. For example, the regular variation of the sound speed with depth leads to

*Agency for Defense Development
국방과학연구소
접수일자 : 1994년 8월 13일

the formation of the underwater sound channel and in sequence, to long-range sound propagation. The random inhomogeneities may cause scattering of sound waves and, therefore fluctuations in the sound field.

From the acoustical point of view, the random inhomogeneities are resulted from currents, internal waves, and small-scale turbulence and cause spatial and temporal fluctuation of the propagating sound. The manuals for sonar operators contain typical SSPs for the area and the time of interest, which shall serve as a proper estimation of sonar conditions. These profiles present an average of available historical data mixed with different environmental conditions. The historical profile can diverge from an actual situation. Hence, the variability of the sound speed in this case cannot be defined as the difference between an actual situation and a historical profile. The constant field may be defined as an average of profiles belonging to the same situation. An ensemble average can be replaced by a temporal or horizontal mean. As a result of the averaging process, random inhomogeneities are smoothed out.

If there exists only internal wave motion which causes variability, the primary profile may be picked from a profile series or it can be calculated by inverse modelling to avoid the unfavorable effects of profile averaging.[2] In most cases, however, internal waves are not the only source of sound velocity variability. Hence, in many cases, even if the amount of measured data is very good, it is difficult to establish a proper definition of the undisturbed sound speed field and to separate it from the fluctuating field.

Historical data usually contain spatial and temporal variations because they have been gathered at many sites for a few hours or days. Even at a fixed point, large variations may occur in SSPs in a short term period.[3] However, there are few data around the Korean Peninsula available to estimate the variability of short term (hourly or less) variations of temperature profiles or SSPs.

This paper examines the hourly variations of temperature profiles in the Korea Strait. In turn, it presents the variability of PL due to the hourly variations of SSPs. Accurate hydrographic measurements were conducted every hour in October, 1993. Currents and meteorological data were measured simultaneously to examine the causes of the variations of temperature profiles. The range-independent PL is calculated using the parabolic equation scheme and averaged over the water depth.

Ⅱ. Hourly variations of temperature profiles

CTD (conductivity, temperature, and depth) castings were performed every hour for 39 hours (12 Oct.-14 Oct. 1993) in the Korea Strait. The water depth is about 198 m and 39 data sets were gathered. CTD was measured by the SBE19 profiler (Sea Bird Electronics Co.). The station is denoted as "M" in Fig.1. Sound speed may be computed from salinity, temperature, and depth where salinity may be converted from conductivity.[4] CTD data can be resolved by less than 10 cm in depth but averaged over every one meter.

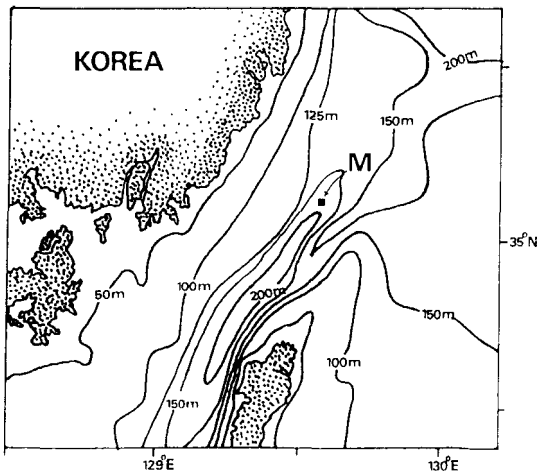

Fig.1 Station map with iso-depth line. The point M is the position where CTD, currents, and meteorological data have been collected during the experiment.

Currents were measured at three depths of 5 m, 57 m, and 190 m for 72 hours (12 Oct. 15 Oct. 1993) using RCM-7 current meter (Aanderaa Instruments Co.). The moored current meters, however, moved up and down severely (up to 25 m) with tidal currents. Hence the current data are excluded from further analysis.

To examine the causes of the hourly variations of temperature profiles, meteorological parameters such as solar radiation, air temperature, and wind speed were measured simultaneously. The measuring instruments for solar radiation and air temperature are MK6 (Matrix Co.) and MR-50 (Hisamatsu Co.), respectively.

Fig.2 shows the time variations of the 39 temperature profiles. Except for some profiles such as number 5 (19:00 Oct. 12) and number 11 (01:00 Oct. 13), they are extended to the bottom where the depth is about 198 m. In the figure, three distinct mixed layers are shown where the surface and the middle layers are shaded. A mixed layer is defined as the layer in which the difference of water temperature is less than 0.2℃ from the first value.[4] The average surface MLD is about 23 m and the layer varies with time from 3 to 43 m. The standard deviation of the surface MLD is as large as 11 m. The depth extent of time variations of profiles is nearly 160 m, 83.3 % of the total water column.

Fig.3 displays the time-depth distributions of temperature and salinity. The X coordinate denotes the time from 11:33 Oct. 12 to 11:09 Oct. 14. In the figure, two events are remarkable in the surface layer. From the event "P" (11:00 Oct. 13), the depth extent of high temperatured water, greater than 20℃, increases linearly for about 4 hours (Fig.3a). The same pattern is shown for that of salinity less than 32.6 ppt for the same period (Fig.3b). It seems impossible for the water mass to be formed there because high tidal currents were experienced (up to 2 kts at 5 m depth) during the experiment. Hence, the water mass is thought to be advected from the neighbouring seas or rivers.

The other event "Q"(22:00 Oct. 14) is characterized by the abrupt changes of temperature and salinity. Namely, the temperature jumps from 20 to 22.8℃ and the salinity from 32.5 to 33.5 ppt. Within one hour, warmer and more saline water mass substitutes for the former one. The water mass falls into the Tsushima Surface Water (TSW), the ranges being 18-25℃ and 32-34 ppt in the Korea Strait in summer.[5] Therefore, it can be said that the modified TSW (due to rainfall or

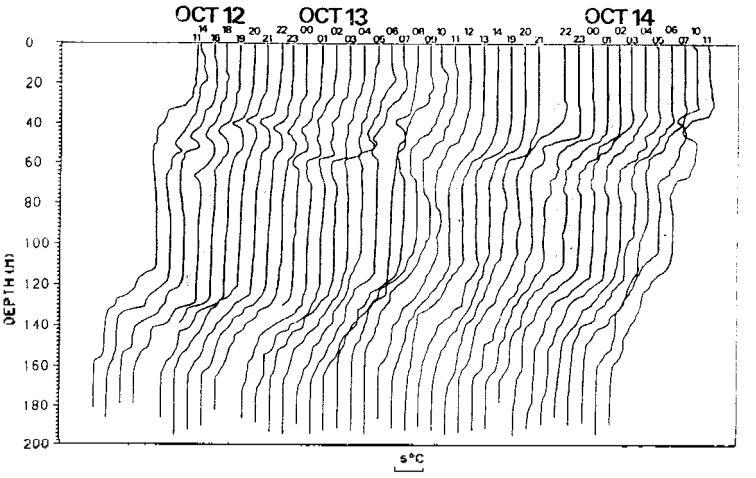

Fig.2 Temporal variation of temperature profiles.

mixing with discharged fresh water from the river) is transported until the event "Q", when the warmer, more saline TSW substitutes for it.

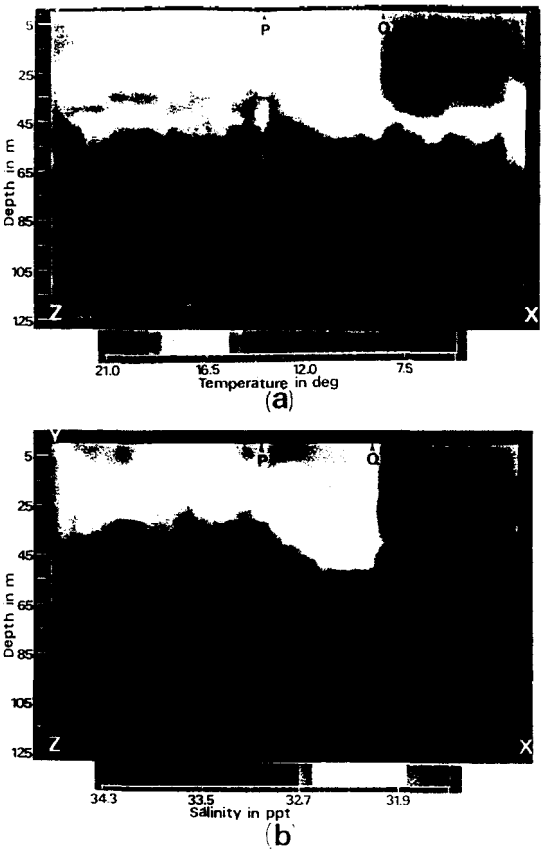

Fig.3 Temporal variations of vertical distributions. The measurement begins at 11 : 33 Oct. 12 and ends at 11 : 09 Oct. 14. (a) temperature, (b) salinity.

Fig.4 shows the relationship between the surface MLD and meteorological data. Measured wind speed (in m/sec) shows no remarkable relation with the surface MLD (Fig.4a). Maximum wind speed is about 12 m/sec. To be fully developed for sea surface wave and thus to be mixed for surface water, strong wind is required for a sufficiently long time.[5] Hence, in order to investigate the relation between a surface mixed layer and wind speed, wind data collection must be started a few days in advance. Before or during the period of experiment, there was no persistent or strong wind. Solar radiation (in watt/m^2) also shows little relationship with the surface MLD (Fig.4b).

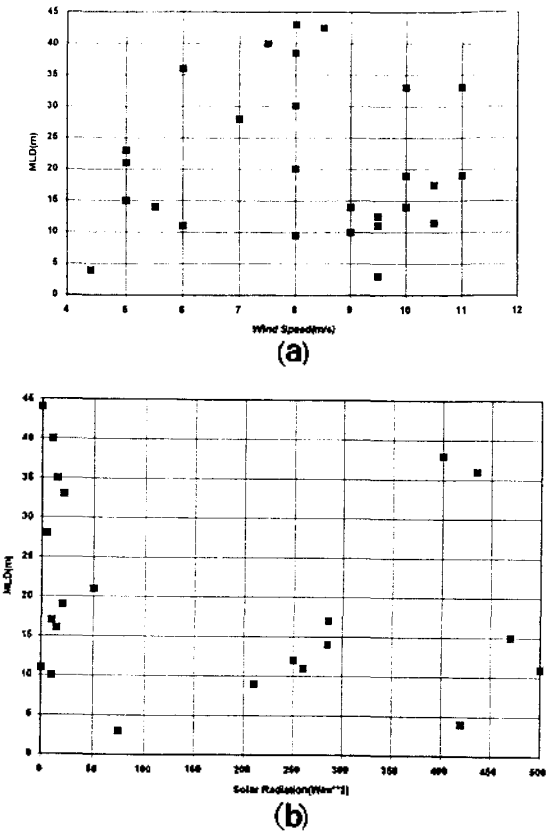

Fig.4 Surface MLD versus meteorological data. (a) wind speed, (b) solar radiation.

Fig.5 shows the time variation of sea surface temperature (SST), air temperature, and salinity. SST and air temperature has no significant relationship. Instead, SST has a strong positive correlation with salinity. Surface mixed layer is very dependent upon heat flux between air and sea, wind stress, surface wave, tidal currents, water mass transport, and eddy.[6-8] In general, surface mixed layer is known to be the strongest in winter and the weakest in summer due to wind stir-

ring and solar radiation around the Korean Peninsula.[4] In a short term period, in addition to wind stirring or solar radiation, water mass movement or tidal currents may also play an important role in the variations of mixed layer in the Korea Strait.

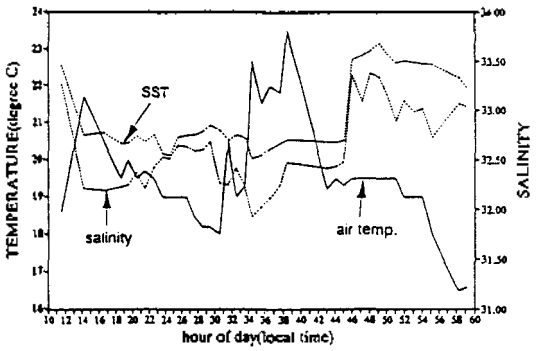

Fig.5 Temporal variations of sea surface temperature (SST), salinity, and air temperature.

Ⅲ. Hourly variation of PL

3.1 Parabolic Equation

We begin with the azimuthally dependent reduced wave equation expressed in cylindrical coordinates (r, θ, z),

$$\nabla^2 P + k_o^2 n^2(r, \theta, z) P = -4\pi\delta(\vec{x} - \vec{x_o}), \tag{1}$$

where $n(r, \theta, z) = c_o/c(r, \theta, z)$: index of refraction,
$k_o = \omega/c_o$: reference wave number,
ω = radian frequency,
c_o = reference sound speed.

For a source at range $r = 0$ and depth $z = z_o$, the delta function is given by

$$\delta(\vec{x} - \vec{x_o}) = \frac{1}{2\pi r}\,\delta(z - z_o)\,\delta(r). \tag{2}$$

We can find a solution of eq. (1) such as

$$P(r, \theta, z) = \sqrt{\frac{2}{i\pi k_o r}}\,\Psi(r, \theta, z)\,e^{ik_o r} = \sqrt{\frac{2}{i\pi k_o r}}\,U(r, \theta, z). \tag{3}$$

where $U(r, \theta, z) = \Psi(r, \theta, z)\,e^{ik_o r}$, $i = \sqrt{-1}$.

In the above equations, $1/r^{1/2}$ models cylindrical spreading while the complex exponential donotes the phase. Subsituting P and its partial derivatives into eq. (7), the wave equation becomes

$$\left(\frac{2}{i\pi k_o r}\right)^{1/2}\left[\frac{\partial^2 U}{\partial r^2} + \frac{\partial^2 U}{\partial z^2} + \frac{1}{r^2}\frac{\partial^2 U}{\partial \theta^2} + \left(k_o^2 n^2 + \frac{1}{4r^2}\right)U\right] = -\frac{2}{r}\,\delta(z - z_o)\,\delta(r). \tag{4}$$

Neglecting all azimuthal scattering and applying far-field approximation ($k_o r \gg 1$), we can discard the terms $\partial^2 U/\partial\theta^2$ and $U/4r^2$. Also since $r > 0$, the right hand side of eq. (4) vanishes. Finally, we obtain the two dimensional wave equation

$$\frac{\partial^2 U}{\partial r^2} + k_o^2 n^2(r, z) U + \frac{\partial^2 U}{\partial z^2} = 0. \tag{5}$$

Substituting $U(r, \theta, z) = \Psi(r, \theta, z)\,e^{ik_o r}$ into eq. (5) yields

$$\frac{\partial^2 \Psi}{\partial r^2} + 2ik_o\frac{\partial \Psi}{\partial r} + \frac{\partial^2 \Psi}{\partial z^2} + k_o^2[n^2(r, z) - 1]\,\Psi = 0. \tag{6}$$

Decomposing Ψ into incoming and outgoing waves, we get

$$\left[\frac{\partial}{\partial r} + ik_o - iQ\right]\left[\frac{\partial}{\partial r} + ik_o + iQ\right]\Psi = 0, \tag{7}$$

where $Q^2 = k_o^2 + k_o^2(n^2 - 1) + \frac{\partial^2}{\partial z^2}$

Considering only the outgoing wave, we obtain the following equation.

$$\left[\frac{\partial}{\partial r} + ik_o - iQ\right]\Psi = 0. \tag{8}$$

Substituting $Q = k_o\left[\frac{A+Bq}{C+Dq}\right]$, $q = \frac{\partial^2}{\partial z^2}$,

we find that

$$\frac{\partial \Psi}{\partial r} = ik_o\left[\frac{A+Bq}{C+Dq} - 1\right]\Psi. \quad (9)$$

According to the selection of coefficients A, B, C, and D, it corresponds to the PEs of Tappert[9] or Claerboat[10]. In this work, the coefficients A=1.0, B=0.75, C=1.0, and D=0.25 (Tappert's) are adopted, which is valid for the ray angles within $\pm 40^\circ$ from the horizontal.

3.2 Model input data

Input data into the model are shown in Fig.6. The sound speed in water is one of the 39 SSPs in Fig.2. It is assumed that the medium consists of three layers (water, sediment, and basement) of which environments are range independent.

The source frequencies are 75 Hz, 150 Hz, and 300 Hz. The source is located at 20 m, 55 m, and 100 m, representing a surface mixed layer, thermocline, and middle mixed layer, respectively. Total of $39\times3\times3=351$ model runs are conducted.

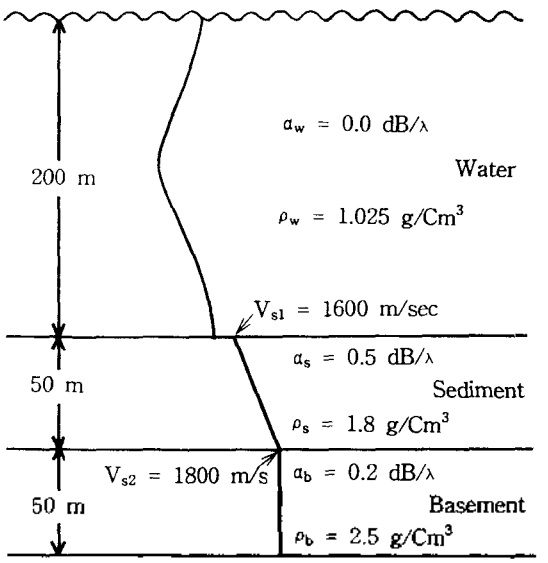

Fig.6 Model input data for the calculation of PL. The SSP in water is one of the 39 SSPs. : attenuation(dB/λ, λ = wavelength), : density(g/Cm^3), V : sound velocity(m/sec).

3.3 Model results

Fig.7 presents the model results for the two cases of SSP : large MLD (10th SSP) and small MLD (20th SSP). The large (small) MLD means that both MLDs of surface and middle are large (small). PL is averaged over water depth in horizontal range of every 200 m. In the figures, relative PL is given. Among the three PL curves for the large MLD (Fig.7a), it can be shown that the PL rate with range decreases as source depth deepens. In the small MLD case (Fig.7b), however, the PL for a source at 100 m becomes larger than that at 55 m beyond 15 km range. In both cases, the PL is the largest at 20 m source depth and the differences among the three PLs reach as large as 10 dB over a 30-50 km range.

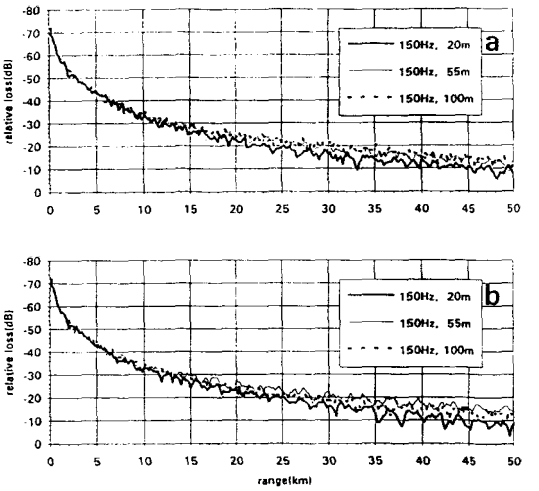

Fig.7 PL comparisons for the two cases of MLD where source frequency is 150 Hz. (a) large MLD(10th SSP), (b) small MLD(20th SSP).

Fig.8 shows the PL variations for the first 10 SSPs. The source, frequency being 150 Hz, is located at 20 m, 55 m, and 100 m. In the figures, it is

obvious that the PL variations reach near 10 dB over a 50 km range. As a whole, the PL variations become larger with increasing range. It can be shown that the PL for a source at 100 m has relatively small variations compared with others.

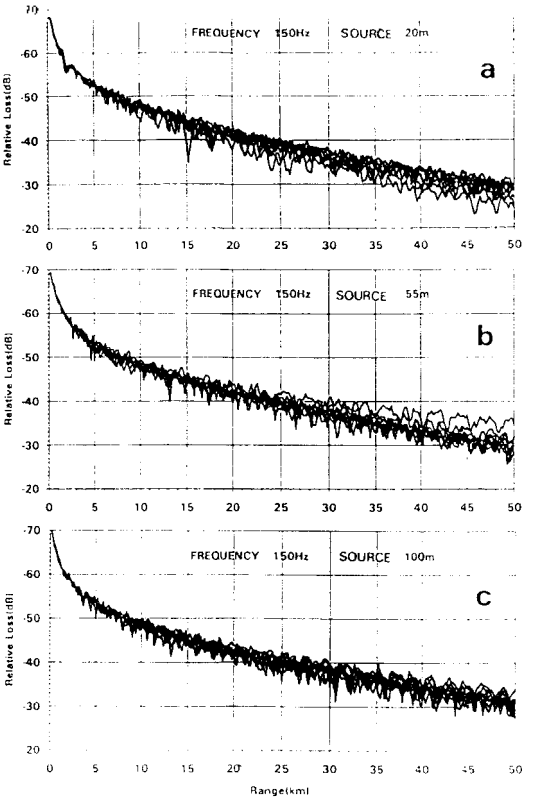

Fig.8 PL variations for the first 10 SSPs with source frequency 150 Hz. (a) source depth 20 m, (b) source depth 55 m, (c) source depth 100 m.

Fig.9 gives the standard deviations of the PL versus range for the frequencies of 75 Hz, 150 Hz, and 300 Hz. In the case of 75 Hz, the two deviation curves for sources at 20 m or 55 m fluctuate but keep on increasing up to near 3 dB as a whole. The deviation for a source at 100 m shows no remarkable increase. It only fluctuates between 1-2 dB over a 20-50 km range. The relatively stable variation (small standard deviation) of the PL for a source at 100 m is comprehensible if one notice two points. The first is the sediment depth that acoustic energy can penetrate. The penetrating depth depends on the frequency of acoustic energy and increases with decreasing frequency. For example, in the shallow water, acoustic energy can penetrate as far as 25 m at 25 Hz while only 6 m at 400 Hz. The second is the temporal variations of SSPs. From Fig.2 or Fig.3, it is clear that the lower layers of the SSPs suffer relatively small variations with time compared with the upper ones. When a low frequency source is at 100 m depth, its acoustic energy may be introduced into the surface of the sediment layer with relatively stable ray paths due to the small temporal variations in the lower layers of SSPs, and then attenuated in the sediment layer. Hence, the two factors lead to the relatively stable variation of the PL for a source at 100 m depth.

In the case of 150 Hz (Fig.9b), the standard deviation for a source at 55 m becomes larger than others from about a 30 km range. The other two deviation curves show no remarkable difference. The large deviations for a source at 55 m are due to the large variations of SSPs around this depth. That is, 55 m depth approximately corresponds to the thermocline in each SSP (Fig. 2) where the temporal variation is the greatest.

In the case of 300 Hz (Fig.9c), it can be seen that the deviation curve is the largest for a source at 55 m and the smallest at 100 m. As a whole, the curve remains within 2 dB, which is smaller than those of 75 Hz and 150 Hz.

In shallow water, the variations of SSPs may have a profound influence on sound propagation over the entire water depth. It may deflect sound wave in water and change the magnitude of bottom interaction. It is shown that the hourly variations of SSPs may cause the depth averaged PL to differ by as much as 10 dB over a 50 km. The standard deviation can reach nearly 3 dB at low frequency. Therefore, in a condition that the PL is critical to estimate the sonar performance, it is suggested that the real time SSPs instead of the

historical ones are essential for the PL calculation.

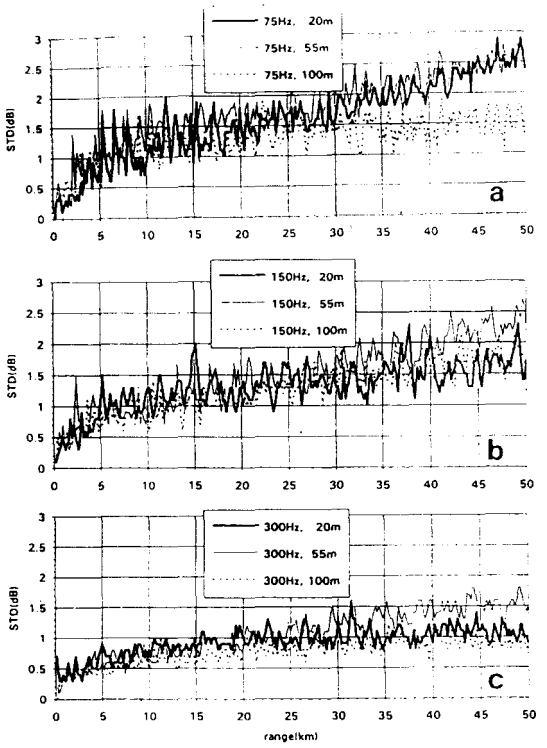

Fig.9 Standard deviations of the PLs for the 39 SSPs. The source depth is located at 20, 55, and 100 m. (a) source frequency 75 Hz, (b) source frequency 150 Hz, (c) source frequency 300 Hz.

Ⅳ. Discussion

The Southeastern Sea of Korea, including the Korea Strait, is known to have very complicated oceanographic environments.[13] That is, there exist various water masses, strong currents, and other phenomena such as thermal fronts, upwelling, and fresh water discharge from rivers. They show very large temporal variations as well as spatial ones. In this work, we casted CTD every hour to estimate the hourly variability of SSPs in the Korea Strait. It is shown that the SSP variations are highly dependent on water mass movement during the experiment. It can be also inferred that the characteristics of incoming water into the specified site may change within an hour and this may cause significant PL fluctuations. If one wants to examine both the spatial distributions of SSPs and the range dependent patterns of PL every hour in concerned area, he or she will find few methods to collect data except remote sensing or air-born expendable bathythermograph.

To verify tens of minutes-scale variations of SSPs like internal waves, one should conduct hydrographic measurements every 5 minutes or less. Internal waves are characterized by scales from 100 m to 1 km or more in the horizontal, 1 to 100 m in the vertical, and from about 10 min to 1 day in time. Internal wave-induced variability has been found to be a very significant source of sound scattering and has received considerable attention in recent years.[14-15] The spatial scales of internal waves match the acoustic wavelength over a broad frequency range, and thereby affect the acoustic field. It is urged that tens of minutes-scale hydrographic and acoustic experiments should be followed for the estimation of the internal wave-induced variability of acoustic field in the concerned sea.

Estimating a variability of the PL, caused by hourly SSP variations, we employed depth-averged one in each horizontal range step. The depth-averaged PL stands for the average PL of the water column between a source and that range. If one considers the temporal variability of PL with a fixed receiver, he or she will necessarily experience much greater fluctuations, and will therefore find it difficult to estimate the PL variability due to SSP variations.

Ⅴ. Summary

The hourly variability of temperature profiles and PL are investigated in this paper. The temperature variations in surface layer show little cor-

relation with wind speed or solar radiation during the experiment. The SSPs are highly variable according to water mass transport from adjacent seas.

The hourly variations of SSPs may cause the depth-averaged PL differ by up to 10 dB over a range of 50 km in the Korea Strait. The variability of PL, represented by standard deviations of the depth-averaged ones, is as large as 3 dB over a range of 50 km. It is suggested that real time SSPs are essential if one wants to compute PL and to estimate sonar performance.

Acknowledgments

We are indebted to Prof. J. Y. Na, Han Yang University and Prof. J. S. Kim, Korea Maritime University for their careful reviews. We wish to thank anonymous referees for their valuable suggestions that greatly improved this paper.

References

1. L. Brekhovskikh and Y. Lysanov, "The Ocean as an Acoustic Medium," in Fundamentals of Ocean Acoustics, Springer-Verlag, 1-31, 1982.
2. D. Rubenstein and M. H. Brill, "Acousic Variability due to Internal Waves and Surface Water," in Ocean Variability & Acoustic Propagation, edited by J. Potter and A. Warn-Varnas, Kluwer Academic Publishers, 215-228, 1991.
3. K. N. Fedrov, "The vertical, horizontal, and temporal scale of the fluctuation of the ocean," in The Thermohaline Finestructure of the Ocean, Pergamon Press, 15-21, 1978.
4. K. Kim, I. S. Oh, and I. S. Kang, "The Mixed Layer Modelling," Agency for Defense Development Report ATRC-408-93791, 1-307, 1994.
5. D. B. Lim and S. D. Chang, "On the cold water mass near Ulsan," J. Oceanol. Soc. Korea, Vol. 13 (2), 5-10, 1969.
6. J. A. Knauss, "Wave Spectrum and the Fully Developed Sea," in Introduction to Physical Oceanography, Prentice-Hall Inc., 210-212, 1978.
7. E. B. Kraus, "Modelling and Prediction of the Upper Layers of the Ocean," Pergaman Press, Oxford, pp. 325, 1977
8. R. C. Thomson, "Climatological numerical models of the surface mixed layer of the ocean," J. Phys. Oceanogr., Vol. 6, 496-503, 1976.
9. A. R. Robinson, "Eddies in Marine Science," Springer-Verlag, New York, pp. 609, 1983.
10. F. D. Tappert, "The parabolic approximation method," in Wave Propagation in Underwater Acoustics, edited by J. B. Keller and J. S. Papadakis, Springer-Verlag, 224-281, 1977.
11. J. F. Claerbout, "Coarse grid calculations of waves in inhomogeneous media with applications to delineation of complicated seismic structure," Geophysics Vol. 35, 407-418, 1970.
12. S. K. Mitchell and K. C. Focke, "The role of the seabottom attenuation profile in shallow water acoustic propagation," J. Acoust. Soc. Am., Vol. 73(2), 465-473, 1983.
13. H. J. Lie and Y. H. Seung, "A Review on Status and Development of Physical Oceanography Research in Korea," J. Kor. Soc. Ocean., Vol. 29(1), 64-81. 1994.
14. Y. Desaubies, "Statistical aspects of sound propagation in the ocean," in Adaptive Methods in Underwater Acoustics, edited by H. Urban, The Netherlands : Dordrecht, Riedel, 1985.
15. B. J. Uscinski, C. Macaskill, and T. E. Ewart, "Intensity fluctuations, Part I : theory, Part II : comparison with the Cobb experiment," J. Acoust. Soc. Am., Vol. 74, 1474-1499, 1983.

▲Young Nam Na
Senior Research Scientist,
Agency for Defense Development
(Vol. 9, No. 6, 1990)

▲Taebo Shim
Chief Research Scientist,
Agency for Defense Development
(Vol. 9, No. 6, 1990)

▲Seong Il Kim
Research Scientist,
Agency for Defense Development
(Vol. 13, No. 3, 1994)